Cell Reports, Volume *27*

Supplemental Information

Metallothionein 3 Controls the Phenotype and Metabolic Programming of Alternatively Activated Macrophages

Debabrata Chowdhury, Hani Alrefai, Julio A. Landero Figueroa, Kathleen Candor, Aleksey Porollo, Roger Fecher, Senad Divanovic, George S. Deepe Jr., and Kavitha Subramanian Vignesh

Supplementary Figures and Figure Legend:

Figure S1:

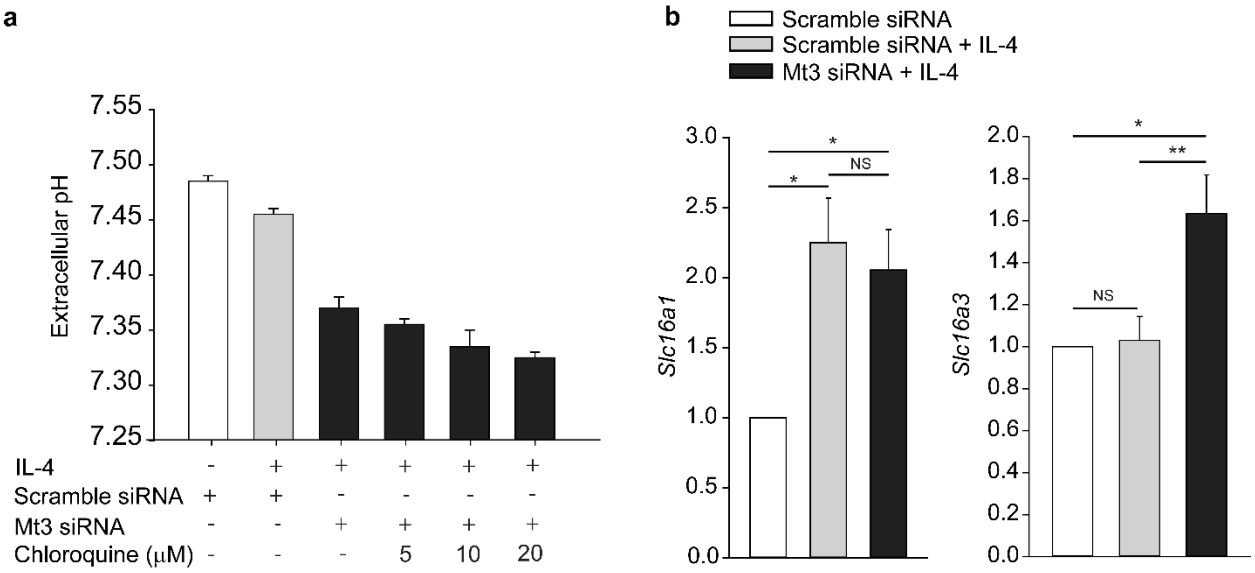

Figure S1: Effect of chloroquine on extracellular acidification and impact of MT3 on lactate transporter gene expression. Related to Figure 2.

(a) Scramble siRNA or Mt3 siRNA treated Mϕ exposed to chloroquine and stimulated with IL-4 for 24 h, 2 independent experiments; and **(b)** Gene expression of monocarboxylic acid transporters *Slc16a1* (MCT1) and *Slc16a3* (MCT4) in *Mt3*$^{-/-}$ Mϕ 24 h post IL-4 stimulation, 5 independent experiments, One-way ANOVA (Holm-Sidak method). Data represent mean ± SEM, One-Way ANOVA, *$p < 0.05$, **$p < 0.01$ and NS, not significant. (See also Figure 2).

Figure S2:

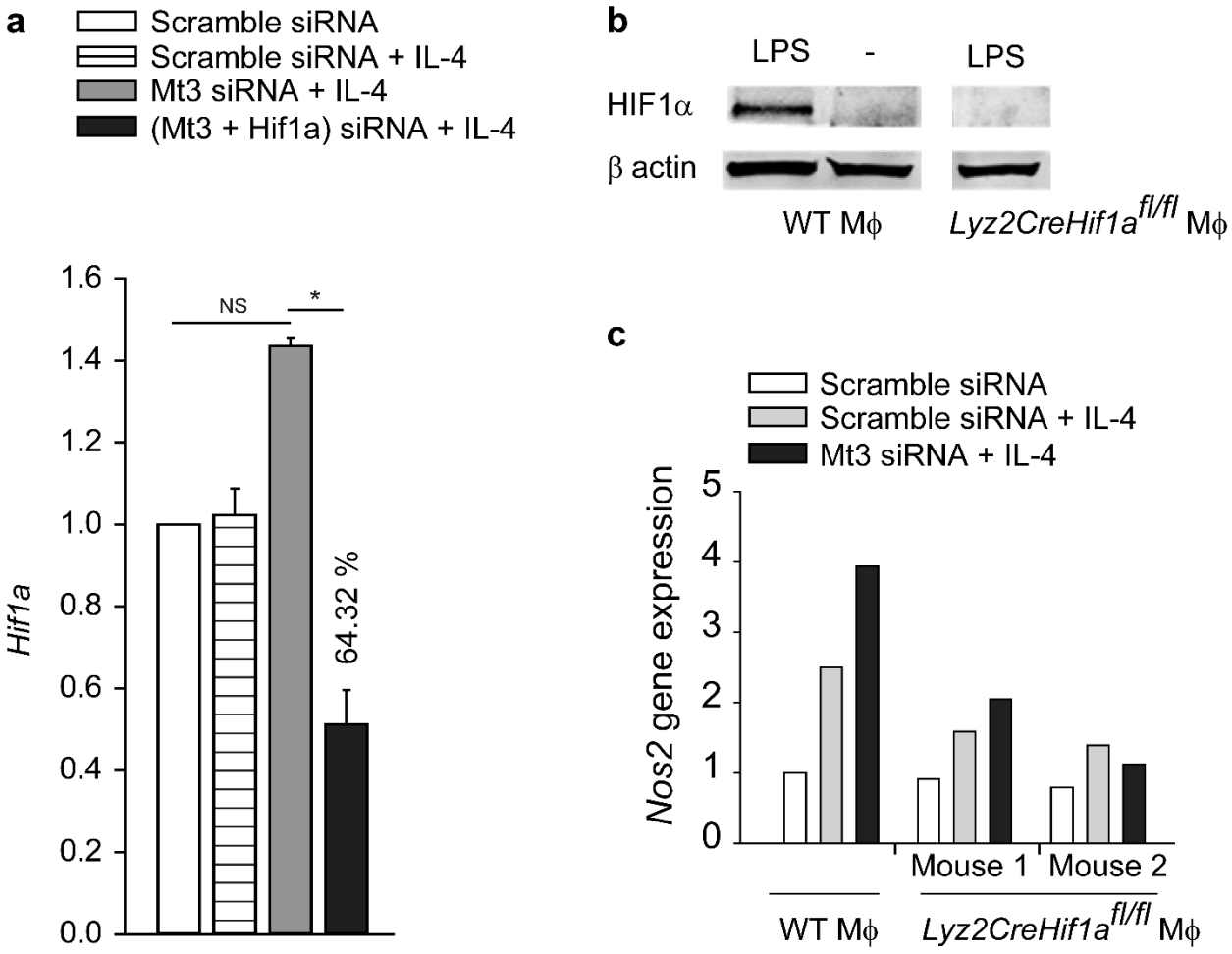

Figure S2: *Hif1a* silencing and analysis of the effect of MT3 in *Lyz2CreHif1a*$^{fl/fl}$ Mϕ. Related to Figure 3.

(a) *Hif1a* expression in M(IL-4) Mϕ treated with either Hif1a siRNA or scramble siRNA control. Percent value represents *Hif1a* silencing in (Mt3 + Hif1a) siRNA treated Mϕ compared to Mt3 siRNA alone; 4 independent experiments, ANOVA on Ranks (Dunn's method), data represent mean ± SEM, *$p < 0.05$ and NS, not significant; **(b)** Western blot of HIF1α from WT and *Lyz2CreHIF1a*$^{fl/fl}$ Mϕ left untreated or treated with LPS (100ng/ml)

for 4h, β actin used as loading control, one representative of 4 independent experiments, the bands are from a single western blot, but the lanes were separated to only present data from relevant samples; **(c)** *Nos2* gene expression in WT and *Lyz2CreHif1a*$^{fl/fl}$ Mϕ treated with scramble or Mt3 siRNA and stimulated with IL-4 for 24h, data from each *Lyz2CreHIF1a*$^{fl/fl}$ mouse is shown separately (See also Figure 3).

Figure S3:

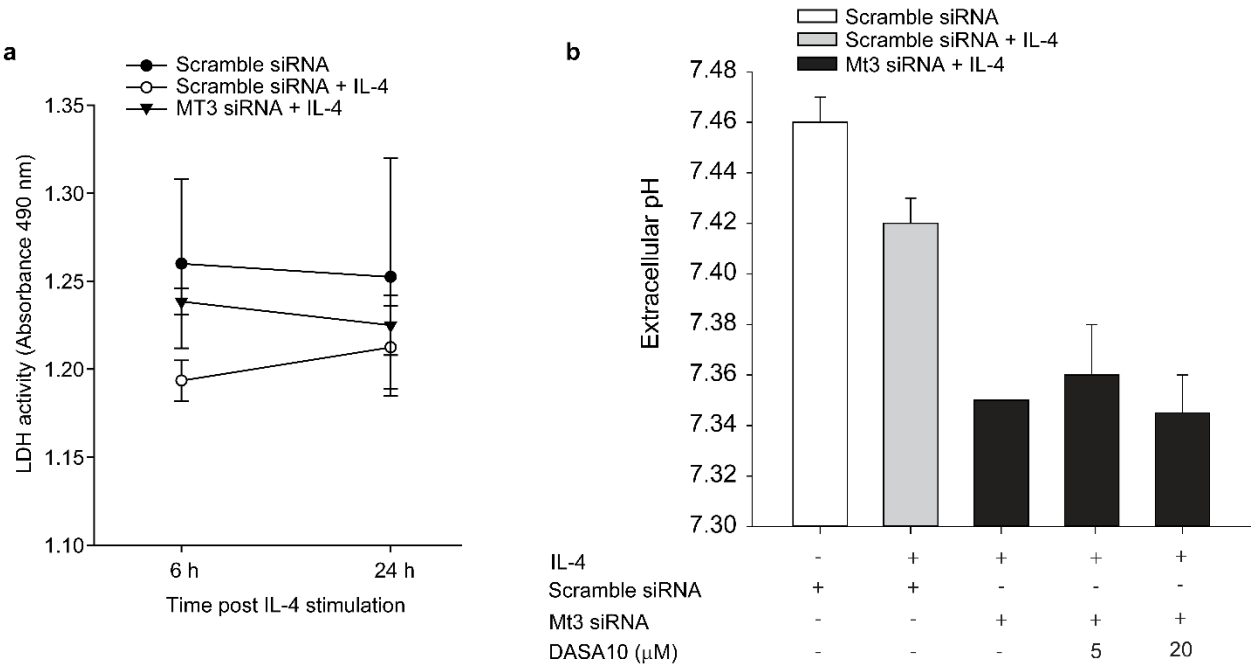

Figure S3: LDH activity in Mϕ and PKM2 activation does not rescue extracellular acidosis in MT3 deficient Mϕ. Related to Figure 4.

(a) Analysis of LDH activity in cell lysates of scramble siRNA or Mt3 siRNA treated Mϕ, 6 h and 24 h post IL-4 stimulation; 2 independent experiments; and **(b)** Extracellular pH in culture supernatants of Mϕ treated with DMSO control or DASA-10 throughout the culture period and stimulated with IL-4 for 24 h; 4 independent experiments, Data represent mean ± SEM. (See also Figure 4).

Figure S4:

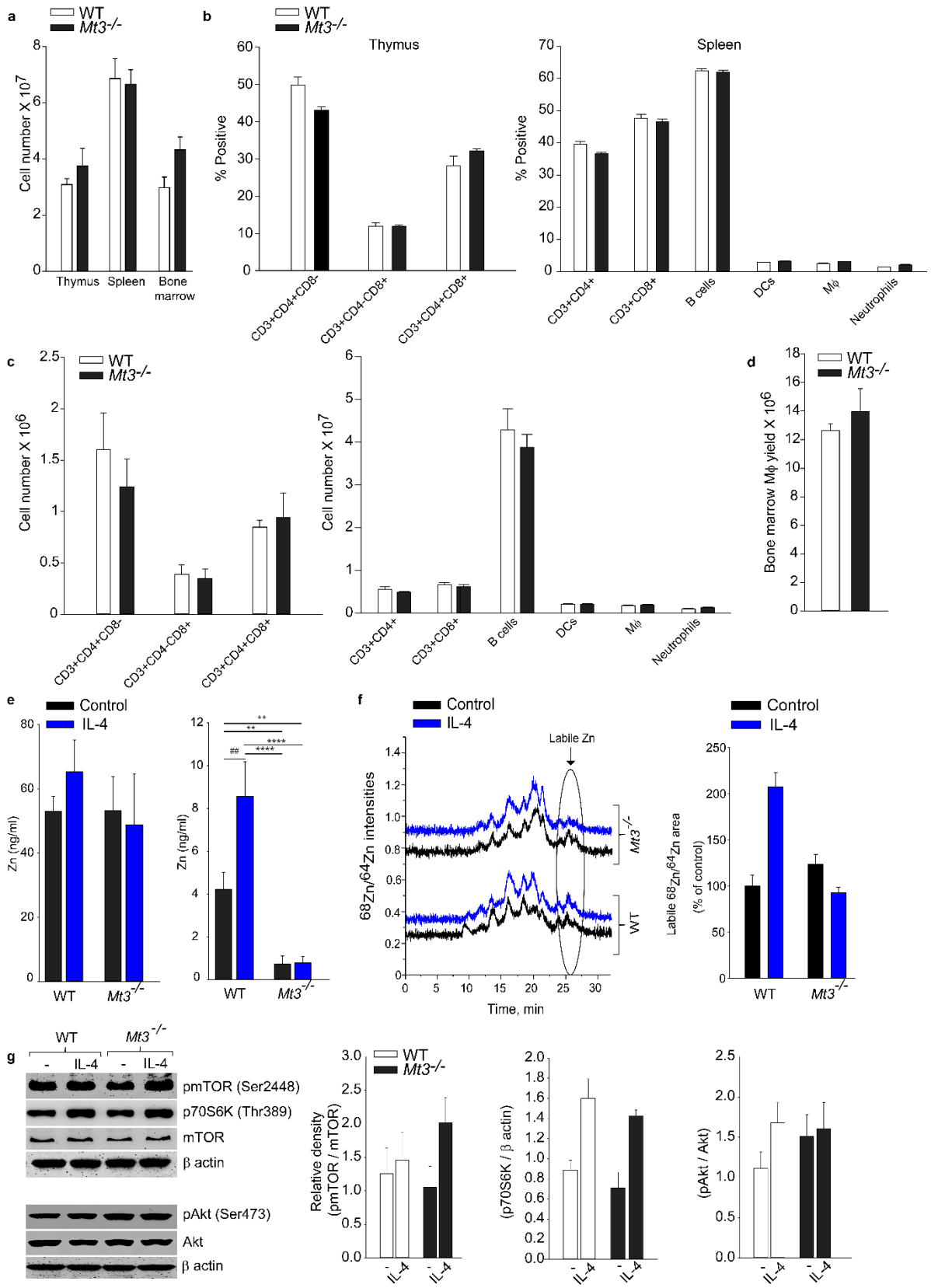
a
WT
Mt3-/-
Cell number X 10^7
Thymus
Spleen
Bone marrow
b
Thymus
% Positive
CD3+CD4+CD8-
CD3+CD4-CD8+
CD3+CD4+CD8+
Spleen
CD3+CD4+
CD3+CD8+
B cells
DCs
Mφ
Neutrophils
c
Cell number X 10^6
Cell number X 10^7
d
Bone marrow Mφ yield X 10^6
e
Control
IL-4
Zn (ng/ml)
f
Labile Zn
68Zn/64Zn intensities
Time, min
Labile 68Zn/64Zn area (% of control)
g
pmTOR (Ser2448)
p70S6K (Thr389)
mTOR
β actin
pAkt (Ser473)
Akt
Relative density (pmTOR / mTOR)
(p70S6K / β actin)
(pAkt / Akt)

Figure S4: Phenotyping of WT and *Mt3*$^{-/-}$ mice, Zn changes and AkT, mTOR activation in WT and *Mt3*$^{-/-}$ Mϕ. Related to Figure 5.

(a) Cell numbers in the thymus, spleen and bone marrow of *Mt3*$^{-/-}$ mice and age-matched wild type (WT) control mice; **(b and c)** Proportion and number of thymic T cells, splenic T and B cells, dendritic cells (DCs), Mϕ, and neutrophils of WT and *Mt3*$^{-/-}$ mice; **(d)** Number of WT and *Mt3*$^{-/-}$ bone marrow derived Mϕ obtained by GM-CSF differentiation, data represent mean ± SEM; **(e)** Size exclusion chromatography-inductively coupled plasma-mass spectrometry (SEC-ICP-MS-MS) analysis of WT and *Mt3*$^{-/-}$ bone marrow derived Mϕ stimulated with IL-4 for 24 h in regular RPMI media, bar graphs show total Zn (left) and labile Zn (right), 3 independent experiments, One-way ANOVA (Bonferroni method); **(f)** SEC-ICP-MS-MS analysis of WT and *Mt3*$^{-/-}$ bone marrow derived Mϕ stimulated with IL-4 for 24 h in ^{68}Zn enriched RPMI media prepared as described (Subramanian Vignesh et al., 2016). Chromatogram on left shows ratio of ^{68}Zn / ^{64}Zn in Mϕ lysates, labile Zn signal (circled region) seen at >25 min in the chromatogram, Y axis, offset for clarity, an increase in ^{68}Zn / ^{64}Zn ratio indicates an elevation in newly imported ^{68}Zn in the Mϕ; bar graph on right shows labile ^{68}Zn / ^{64}Zn ratio in untreated and IL-4 treated WT and *Mt3*$^{-/-}$ Mϕ. The data show that IL-4 fails to elevate labile ^{68}Zn / ^{64}Zn ratio when MT3 is absent, data represent mean ± SD, 2 independent experiments; and **(g)** Western Blot of pAkt, Akt, pmTOR, mTOR, p70S6K and β-actin in total cell lysates of WT and *Mt3*$^{-/-}$ Mϕ 24 h post IL-4 stimulation, pAkt, pmTOR and p70S6K were normalized to Akt, mTOR and β-actin respectively, 3 independent experiments (See also Figure 5).

Figure S5:

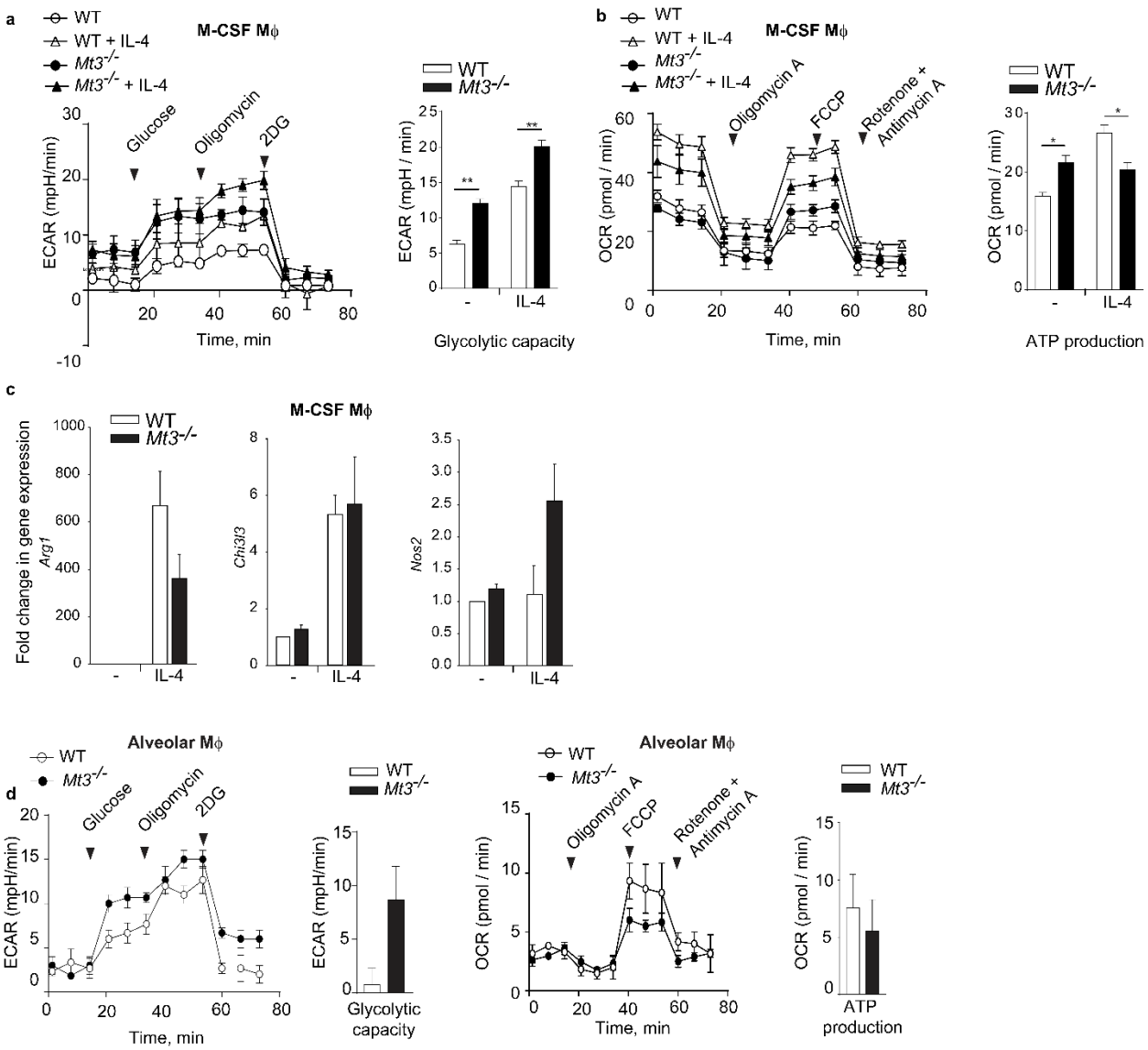

Figure S5: MT3 regulates Mϕ metabolism in M-CSF derived Mϕ and in alveolar Mϕ. Related to Figure 5.

(a and b) ECAR and OCR plots of bone marrow derived WT and *Mt3*$^{-/-}$ Mϕ differentiated using M-CSF, followed by no treatment or stimulation with IL-4 for 24 h, bar graphs (right)

show ATP production and glycolytic capacity, 3 independent experiments, One-way ANOVA (Tukey method); **(c)** Gene expression analysis of *Arg1, Chi3l3* and *Nos2* in WT and *Mt3*$^{-/-}$ M-CSF derived Mϕ left untreated or treated with IL-4 for 24 h; and **(d)** ECAR and OCR plots of alveolar Mϕ from WT and *Mt3*$^{-/-}$ Mϕ, bar graph (right) shows ATP production and glycolytic capacity, 3 independent experiments; two-way ANOVA (Holm Sidak method); data represent mean ± SEM (See also Figure 5).

Figure S6:

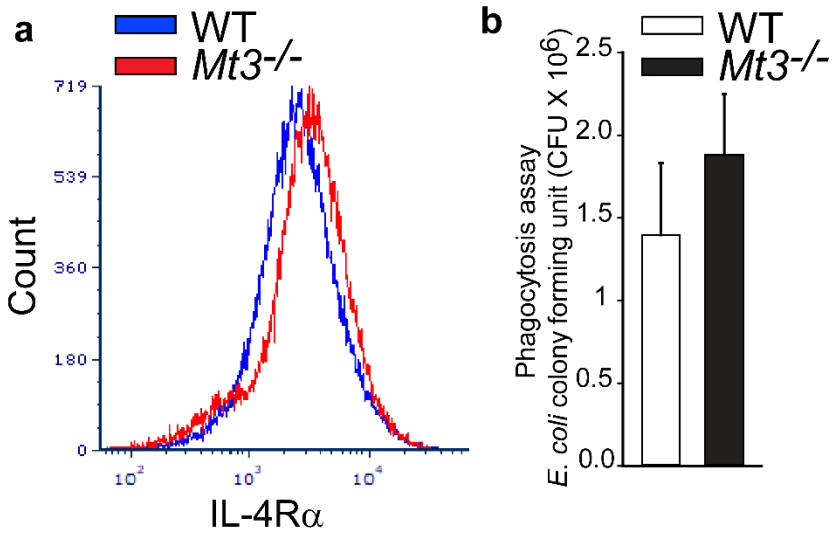

Figure S6: IL-4Rα expression in *Mt3*$^{-/-}$ Mϕ and *E. coli* phagocytosis. Related to Figure 6.

(a) Dot plots showing IL-4Ra expression in WT and *Mt3*$^{-/-}$ Mϕ at baseline, 3 independent experiments; and **(b)** Phagocytosis of *E. coli* K12 by WT and *Mt3*$^{-/-}$ Mϕ 3.5 h post infection, data are presented as CFU, 4 independent experiments. Data represent mean ± SEM. (See also Figure 6).